HHS Public Access

Author manuscript

Wound Repair Regen. Author manuscript; available in PMC 2018 April 27.

Published in final edited form as:

Wound Repair Regen. 2017 April ; 25(2): 177–191. doi:10.1111/wrr.12516.

Regeneration of injured skin and peripheral nerves requires control of wound contraction, not scar formation

Ioannis V. Yannas, **Dimitrios S. Tzeranis**, and **Peter T. C. So**

Departments of Mechanical and Biological Engineering, Massachusetts Institute of Technology, Cambridge, MA 02139

Abstract

We review the mounting evidence that regeneration is induced in wounds in skin and peripheral nerves by a simple modification of the wound healing process. Here, the process of induced regeneration is compared to the other two well-known processes by which wounds close, i.e., contraction and scar formation.

Direct evidence supports the hypothesis that the mechanical force of contraction (planar in skin wounds, circumferential in nerve wounds) is the driver guiding the orientation of assemblies of myofibroblasts (MFB) and collagen fibers during scar formation in untreated wounds. We conclude that scar formation depends critically on wound contraction and is, therefore, a healing process secondary to contraction.

Wound contraction and regeneration did not coincide during healing in a number of experimental models of spontaneous (untreated) regeneration described in the literature. Furthermore, in other studies in which an efficient contraction-blocker, a collagen scaffold named dermis regeneration template (DRT), and variants of it, were grafted on skin wounds or peripheral nerve wounds, regeneration was systematically observed in the absence of contraction. We conclude that contraction and regeneration are mutually antagonistic processes.

A dramatic change in the phenotype of myofibroblasts was observed when the contraction-blocking scaffold DRT was used to treat wounds in skin and peripheral nerves. The phenotype change was directly observed as drastic reduction in MFB density, dispersion of MFB assemblies and loss of alignment of the long MFB axes. These observations were explained by the evidence of a surface-biological interaction of MFB with the scaffold, specifically involving binding of MFB integrins $\alpha_1\beta_1$ and $\alpha_2\beta_1$ to ligands GFOGER and GLOGER naturally present on the surface of the collagen scaffold.

In summary, we show that regeneration of wounded skin and peripheral nerves in the adult mammal can be induced simply by appropriate control of wound contraction, rather than of scar formation.

Conflict statement

I.V. Yannas has participated in the founding of Integra LifeSciences, Plainsboro, NJ. He currently has no financial connection with the company and owns no stock of Integra LifeSciences.

Introduction

Injury to an organ generates a wound and is normally followed by a spontaneous (untreated) healing process at the end of which a healthy wound has closed. In the adult mammal, injury to the stroma is typically irreversible and eventually leads to formation of scar, a nonphysiological tissue (repair). Regeneration of stroma, i.e., recovery of the structure and function of the original tissue, is typically not observed.

The clinical consequences of such irreversible healing processes are enormous since they often cause loss of function in vital organs.(1) Scar formation has been frequently cited as a physical and chemical barrier for regeneration, particularly in studies of regeneration of axons in the injured central nervous system. (2–4) However, in studies with wounds in skin and peripheral nerves, substantial evidence has been presented showing that scar formation can be cancelled and regeneration achieved by appropriate modification of the wound healing process, specifically blocking of the normal wound contraction process. (5) Because of the striking importance of the medical consequences of wound healing it appears worthwhile to explore the connection between wound healing and regeneration. We provide below background evidence that leads to an understanding of such a connection.

In this review the wound healing process is viewed in terms of the relative contribution of the macroscopic processes by which an injured organ achieves the end state of wound closure. We have emphasized the viewpoint of the end state (closure) of the wound healing process, rather than its intermediate mechanism (involving an often bewildering host of biochemical and cell biological interactions), because wound closure occurs by a small number of processes, namely, contraction, scar formation and regeneration. Each of these processes is well-defined and their respective quantitative contributions to wound closure can be determined by measuring the fraction of standardized wound area that has closed by each process. The relationships among them can be evaluated using appropriate wound healing models that emphasize one or the other of these processes. Extensive quantitative data on the three processes of wound closure have so far been sparse; however, there is sufficient information currently to introduce this viewpoint. For example, dermis (the outcome of a regeneration process) and scar can be quantitatively distinguished using laser scattering from histological slides, as illustrated in Fig. 1.

Evidence is presented in this review that is used to evaluate qualitatively the relative importance of each of the three processes of wound closure in healing of well-defined wounds in two organs, skin and peripheral nerves. This approach eventually identifies a useful pathway, presented at the cell-biological scale and supported by a molecular mechanism, that leads to cancellation of scar and induction of regeneration.

Relation between Wound Contraction and Scar Formation

In the section below skin wounds studied were full-thickness dorsal skin wounds in rodents. Unimpaired, acute skin wounds, not chronic wounds, were only included. (However, there is a pointed reference to chronic skin wounds at the end of the next section) The peripheral

nerve wound studied was the fully transected sciatic nerve of the rat. Both of these animal models have been used extensively in the literature of wound healing.

We start our analysis with a description of the formation of dermal scar in a rodent wound healing model. Synthesis of dermal scar has been described in a detailed series of light photomicrographs and ultrastructural images observed in healing of skin wounds in the guinea pig (6). In this study the development of connective tissue morphology following wound healing was studied both in the presence and absence of a collagen scaffold with highly specific structure (dermis regeneration template, DRT). The latter is known for its unusual property of strongly delaying or blocking wound contraction in skin wounds (7,8) and peripheral nerve wounds. (9) DRT also induces regeneration of the dermis and the peripheral nerve trunk in several adult mammalian species, (7,8,10) including the human. (11) In the full-thickness untreated (DRT-free) skin wound, used as a negative control which contracts normally, the long axes of highly elongated fibroblasts were observed to be aligned parallel to the epidermal (wound) plane, both in the superficial and deep dermis, by day 14 post injury. By 1 year fibroblasts deposited similarly oriented, coarse collagen bundles, resembling scar. The presence of scar was confirmed by observing a flat dermal-epidermal junction. In contrast to the above, when the skin wound had been grafted with DRT, the fibroblasts observed on day 14 were fusiform to stellate in shape, rather than highly elongated, and their axes were randomly oriented in space rather than being aligned in the plane. By 1 year, these fibroblasts were associated with delicate, interwoven collagen bundles, resembling normal dermis. (6) In summary, in these sequences of light microphotographs and ultrastructural images, the long axes of fibroblasts in untreated healing skin wounds were shown to be oriented in the plane of the wound and collagen fibers synthesized in these wounds were also oriented in the same plane. In contrast, fibroblast axes in wounds treated with contraction-blocking DRT were randomly oriented in space and synthesis of collagen fibers in the DRT-treated wounds yielded randomly oriented collagen fibers. (6) We seek below an explanation for these data.

Deeper insight into the origin of scar formation is gained when fibroblasts in the healing skin wound or peripheral nerve wound are stained by use of an antibody for alpha smooth muscle actin, which is specific for myofibroblasts (MFB). These differentiated fibroblasts have been credited with generating almost all the contractile forces and resulting tissue deformations in skin wounds. (12–16) Although other actin isoforms, such as smooth muscle γ-actin and skeletal muscle α-actin, have been implicated in force generation, (17) the alpha smooth muscle actin isoform is currently considered by many authors to be the most used marker of the myofibroblastic phenotype. (18) These cells are highly elongated and display densely bundled actin microfilaments at their perimeter. One of the most widely recognized phenotypes of myofibroblasts are “stress fibers”, prominent filaments containing alpha smooth muscle actin. (12,19) Expression of the myofibroblast phenotype has been shown to require the presence of transforming growth factor beta1 (TGFβ1), a fibronectin fragment, and mechanical tension. (19) Following wound closure, myofibroblasts disappear by apoptosis. (20,21) The axes of myofibroblasts have been shown to adopt a preferred alignment in the plane of spontaneously healing skin wounds and circumferential alignment around peripheral nerve stumps wounded by transection (see below). Myofibroblast assembly and orientation was clearly observed in tissues from an untreated, spontaneously

contracting full-thickness dorsal skin wound in the guinea pig following staining with the alpha smooth muscle actin antibody (Fig. 2, *top*). (5) Expression of the gene for alpha smooth muscle actin by a variety of connective tissue cells of the musculoskeletal system has been reviewed. (22) The requirement for a myofibroblast mechanism in skin wound contraction has been occasionally disputed. (23–27)

The mechanical field acting on myofibroblasts in a full-thickness skin wound that heals spontaneously by contraction and scar formation will now be considered. An approximate description of the mechanical field is plane tensile stress, similar to the stresses experienced by a thin sheet which is being stretched by forces in the plane of the sheet. In the contracting skin wound these stresses stretch the skin present outside the wound perimeter in a direction toward the wound interior (centripetal direction). The two normal stresses in the plane of the wound are usually unequal in magnitude and the resulting deformation is maximal along the direction of the larger stress component (major deformation axis; see (28)).

The orientation (alignment) of myofibroblasts in the space of the wound appears to be strongly affected by the presence of the mechanical field in which the fibers are synthesized. A similar physical phenomenon has been long recognized in the field of mechanics of synthetic polymer mechanics (e.g., alignment of long macromolecular crystallites following extrusion of textile fibers from a spinneret, followed by stretching). The fibers synthesized by the cells are also aligned in an apparently similar manner. It has been previously shown that fibroblasts deposit newly synthesized collagen fibers in a direction approximately parallel to their own long cell axes. (29) In the full-thickness guinea pig skin wound (untreated), direct observation of the cells that had expressed the alpha smooth muscle actin phenotype, and were ultrastructurally identified as myofibroblasts, showed that the long axes of these cells were oriented in the plane of the wound surface; out-of-plane orientation of axes of MFB was negligible.(6) Confirmation of high myofibroblast alignment in the same untreated animal model was provided in a skin wound that was undergoing vigorous contraction on Day 10 following injury (Fig. 2, *top*). A high magnification view of tissue from Fig. 2, *top* is shown in Fig. 3A, *left*. This latter microscopic view confirms the MFB alignment in the plane of the untreated skin wound. We recall earlier findings in a quantitative study of histological sections from skin wounds by laser light scattering that showed newly synthesized collagen fibers in guinea pig scar being aligned in the plane of the epidermis and along the major deformation axis of the contracting wound.(30) Alignment of collagen fibers in dermal scar has been previously reported in numerous independent studies. (31–34) An example of the major deformation axis during skin wound closure has been described.(30) We conclude that there is wide agreement in the literature that scar in healing skin wounds is a tissue characterized by high alignment of collagen fibers in the plane of the wound.

In peripheral nerve wounds, during healing of the transected rat sciatic nerve, and in the absence of tubulation often used to connect the nerve stumps (untreated control), myofibroblasts were observed in a state of circumferential alignment around the regenerate 14 days post-injury (Fig. 3B, left). A study of the mature healed nerve, obtained in a lengthy 60-week study, using the silicone elastomeric tube as a conduit connecting the stumps (which, like the tubeless control, also allows extensive contraction to take place), showed

MFB in a circumferential alignment around the nerve stump, forming 15–20 myofibroblast layers (often referred to in the literature as a contractile capsule). (35)

The evidence shows that neural scar is largely made up of collagen fibers that are aligned circumferentially around the stump resulting from transection. An image of the transected peripheral nerve model that had been obtained at 9 weeks following treatment with a poorly regenerative analog of the DRT (member of a collagen library of DRT analogs, see below), showed collagen fibers wrapped around the circular cross section of neural tissue and exhibiting their clearly circumferential orientation (Fig. 4A). (9) Since the MFB layer surrounding the neural tissue was also shown to be circumferential (see Fig. 3B *left*; also (35)), the evidence in Figs. 3B *left* and 4A supports further the early general finding that, during collagen synthesis, fibroblasts deposit newly synthesized collagen fibers in an alignment that parallels the orientation of cell axes. (29).

Evidence supporting compression of the cross section of the nerve stump during healing was obtained using collagen scaffolds that were closely matched in structure to DRT but had shown diminished ability to block contraction and induce regeneration or had altogether failed to block contraction and were also regeneratively inactive.(9,36,37) The five scaffold members, labeled A through E, differed only in the increasing level of crosslink density along the series, with scaffold E being the most highly crosslinked. Images of the regenerate obtained by two-photon microscopy at 9 weeks showed a neural tissue diameter of about 400 μm when scaffold tube E, which allowed contraction, was used (Fig. 4B, *left*). However, neural tissue diameters of about 1000 μm or higher were measured when scaffold tube D (fabricated from contraction-blocking DRT) was used (Fig. 4B, *right*). (The physiological nerve diameter for this animal model is about 850 μm. Regenerating nerves typically measure neural tissue diameters larger than normal for several weeks after tubulation; see detailed evidence in (35)) The difference in diameter between the two regenerating nerves shown in Fig. 4B *left, right* can most simply be explained by the presence of contractile forces that induce a differential compressive deformation (shrinking) along the radial axis (major deformation axis) of the nerve trunk.

Quantitative evidence supporting the hypothesis of compressive shrinkage of the regenerating nerve trunk was obtained in a study with the transected rat sciatic nerve where the diameter of the healing nerve was shown to decrease with increasing thickness of the myofibroblast capsule surrounding the nerve (Fig. 5, *left*).(9) In the five groups of animals, each treated with scaffolds A through E along a series that comprised members with increasing crosslink density, the thickness of the MFB capsule exhibited gradually increasing values (suggesting an increasing compressive force along the series) following treatment with the members of this internally controlled scaffold library. The data in Fig. 5, *left* are most simply interpreted as increasing shrinkage of the stump diameter resulting from a compressive stress field applied by an increasingly thick myofibroblast capsule. (9) This explanation is consistent with a linear elastic model of radial compressive strain which varies directly with the thickness of the contractile cell capsule.(9)

A simple analogy of the contractile mechanical field acting around the nerve regenerate is squeezing of a person’s arm following application of a pressure cuff for measuring blood

pressure. This analogy has defined the “pressure cuff” theory of peripheral nerve regeneration across a long gap formed by nerve transection. (38) The theory explains the low quality of PN regeneration, frequently observed in several experimental configurations in the literature: Shrinkage of the diameter of neural tissue resulting from compression by the MFB capsule is accompanied by decrease in number of myelinated axons in the reduced cross section (Fig. 5 *right*), resulting in morphology that is characteristic of a peripheral nerve with increasingly poor fun*ctio*nal properties. This simple theory has explained qualitatively a large number of independent data in the field of peripheral nerve regeneration using a variety of tubes that were studied as conduits connecting the stumps. (38) In summary, we theorize that the myofibroblasts shown to be aligned circumferentially around healing nerve stumps (Fig. 3B *left*; also (35)) apply compressive stresses (“hoop stresses”) that result in the observed shrinking of the nerve along its radial axis (Figs. 4B, Fig. 5 *left*) thereby impeding regeneration of the original morphology. We conclude that circumferentially aligned MFB synthesize collagen fibers with similar circumferential alignment (Fig. 4A), leading to formation of neural scar around the nerve stump.

The combined observations cited above lead to a conclusion that applies both to skin wounds and nerve wounds. During normal contraction of the untreated wound, collagen fibers are observed to be deposited in an alignment that coincides with that of the MFB long axes, themselves being in alignment with the major deformation axis of the mechanical field. The outcome of this process is synthesis of collagen fibers in a pattern consistent with a scar-like stroma which appears to be a close topographic replica of the cellular (myofibroblast) configuration in the contracting wound. These observations on MFB alignment lead to a useful analogy between contracting skin wounds and peripheral nerve wounds: The geometry of contraction of skin wounds appears to differ from that in peripheral nerve stumps primarily with respect to differences in the macroscopic topographical anatomy of the two organs (rather than differing in detailed cell-biological details), which is planar in skin and cylindrical in nerves.

The evidence presented above has led to a deformation field theory of scar formation in skin wounds and peripheral nerve wounds: The mechanical field that drives physiologic wound contraction in each injured organ theoretically controls the alignment of contractile cells in the wound. The mechanical field is approximated as plane tensile stress in skin wounds and circumferential compression in nerve wounds. Alignment of cells eventually leads to synthesis of collagen fibers with similar alignment and ultimately results in the characteristic fiber alignment observed in dermal and neural scar. The deformation theory of skin scar and neural scar formation has been described. (5) We present a simple schematic representation of this theory for spontaneously healing skin wounds and peripheral nerve wounds (Fig. 6). The schematics for these two different organs are closely based on the data shown in the photos (see figure legends for details).

A necessary consequence of the deformation field theory of scar formation is that the alignment both of long MFB axes and of newly synthesized collagen fibers should be cancelled when the mechanical field of wound contraction becomes inactive, leading to MFB and corresponding collagen fibers that lack a preferred alignment. Direct experimental support for this prediction, both from skin wounds (Fig. 3A, *right*) and peripheral nerve

wounds (Fig. 3B, *right*), was obtained following use of the contraction-blocking collagen scaffold, DRT. The photographic evidence shows loss of alignment both in skin wounds and peripheral nerve wounds in the presence of DRT. Although DRT was originally discovered in connection with its regenerative activity, (7,10) the discussion is focused instead here on the unique information that this efficient contraction blocking agent provides when used as an experimental probe. Evidence for the contraction-blocking activity of DRT in skin wounds has been presented in earlier studies where it was shown that macroscopic wound contraction was either very strongly delayed or arrested in the presence of DRT. (8,9) We conclude that the evidence supports the prediction of the deformation theory: contraction-blocking DRT cancels the alignment of collagen fibers characteristic of scar.

We now consider the temporal relationship between the wound healing processes of contraction and scar formation. During spontaneous healing, contraction appears first, followed much later by scar or regeneration. For example, in a study of the untreated guinea pig skin wound, the wound started contracting no later than 3–4 days after injury while approximately 50% of the wound area had closed by contraction by day 10 and complete wound closure was observed approximately by day 35. (8) By day 10, a well-developed layer of aligned myofibroblasts had already been established while the wound was contracting vigorously. In the same animal model, there was no evidence of scar formation by day 14 either in the superficial or deep dermis. (6) Although the documentation was sparse, clear evidence of scar appeared a few weeks after injury, at about approximately the same time that the wound was closing or had closed by contraction. (6) In the transected peripheral nerve, alignment of myofibroblasts was evident by day 14 (Fig. 2B, left) and MFB persisted even at 60 weeks. (35) MFB first appeared in peripheral nerve wounds as early as approximately 7 days (data not shown here). Definitive neural scar both in the proximal and distal stumps had appeared by 6 weeks, (35) and probably earlier. The conclusion from the data, both with skin and peripheral nerve wounds, is that contraction starts clearly earlier than does scar formation. The sequence of scar-forming events appears to be as follows: Contraction sets up a mechanical field > MFB become oriented in mechanical field > Collagen synthesis occurs by oriented MFB > Scar forms.

We turn next to the evidence concerning the mutual dependence of contraction and scar formation processes. Although contraction appears before scar formation, the data with mammalian wounds discussed above do not address the provisional hypothesis that the processes may nevertheless have a common origin and are expressed together rather than being independent of each other. This question was answered in a quantitative study of spontaneous closure of skin wounds in the tadpole, the early form of a frog species, as well as in the adult frog. (39) Although the tadpole is an anuran, there appears to be no evidence that the basic wound healing processes in tadpole skin are qualitatively different than those in mammals. The absence of scar in the tadpole model was confirmed histologically through the entire developmental cycle of the tadpole; scar made its first appearance after metamorphosis of the tadpole to the adult frog had occurred. Tadpole skin wounds closed both by contraction and regeneration, with persistent absence of scar, and in relative magnitudes that varied through development. The readily measurable magnitude of contraction increased while regeneration correspondingly decreased during tadpole development. (39) In this study absence of scar clearly did not lead to cancellation of

contraction, indicating that changes in the magnitude of contraction were observed independently of the presence of scar. This finding contradicts the provisional hypothesis that the two processes, contraction and scar formation, have a common origin and hypothetically are expressed in parallel.

The conclusions from the data describing the mutual dependence of contraction and scar formation is that contraction in skin wounds and peripheral nerve wounds starts clearly earlier than does scar formation. Scar synthesis follows development of the mechanical field of wound contraction which orients the cells (MFB) that synthesize collagen fibers with the characteristic orientation pattern of scar. Furthermore, contraction can take finite values while scar persists at zero (tadpole data; (39)). The data can be best explained by concluding that scar formation is a process secondary (derivative) to wound contraction. It follows that scar formation can be prevented simply by early application of contraction blocking. Therefore, in studies where the use of a DRT graft led to cancellation both of contraction and scar, blocking of contraction by DRT is predicted to have sufficed to cancel scar formation as well.

An antagonistic relation between wound closure by contraction and by regeneration

In this section, evidence on spontaneously healing (untreated) skin wounds is cited from studies with a variety of species (rabbit, mouse, swine, axolotl), providing a set of data that naturally point to an antagonistic relation between contraction and regeneration. A second set of data, pointing to a similar conclusion, was obtained with DRT-treated wounds in rodents (skin wounds were full-thickness; peripheral nerves were the transected rat sciatic nerve).

We summarize first independent evidence of scarless healing from diverse species where contraction and regeneration did not occur together, or else coexisted in competition with each other. We consider the well-known example of skin wounds in the perforated rabbit ear where wound contraction has been clearly shown to be excluded due to tight binding between skin and underlying cartilage, (40) and where regeneration, or scarless healing, of skin is observed. (41–45) In contrast, injury in a different anatomical site of the same species (dorsal wound in rabbit) showed the commonly observed result that skin wounds closed with an estimated contraction of 96% of initial wound area, the remainder being scar. (46) In a quite different anatomical site, studies of healing of the injured oral mucosa in mice showed greatly reduced scar formation or even scarless healing. (47–51) In studies of scarless healing of oral mucosal wounds with swine it was shown that these wounds contracted significantly less than in skin wounds of the same species (48) or else showed lower levels of TGFβ1 (cytokine required for expression of the alpha smooth muscle actin phenotype in fibroblasts) than in control skin wounds. (47) The axolotl is a urodele amphibian with unique ability among vertebrates to regenerate lost appendages (limbs, tail) and other body parts, including heart, forebrain and jaw. (52) Full-thickness excisional skin wounds in the axolotl led to the expected spontaneous regeneration of the skin (53) while a separate study of similar skin wounds in the axolotl showed that alpha smooth muscle actin, a protein

characteristic of contractile cells, was absent and that TGFβ1 was only transiently expressed during wound healing. (52,54) We also cite quantitative data from a study of the developing tadpole (described in the preceding section) where, in the absence of scar formation, contraction and regeneration do occur together yet appear as mutually exclusive processes of skin wound closure. (39) The data in the latter study showed that, during the entire four stages of tadpole development, the fractional contribution of contraction to wound closure increased from about 41 to 90% while the contribution of regeneration simultaneously fell from about 59% to 10%, with scar persisting at zero levels throughout tadpole development. The experimental evidence in each of these studies with skin wounds in various species that heal spontaneously without scar formation has led to the conclusion that scarless healing (regeneration) of these wounds was persistently observed coincidentally with the absence of wound contraction. In one instance (tadpole), scarless healing was observed to coexist in competition with contraction for wound closure.

A second set of data that independently supports an antagonistic relation between wound contraction and regeneration includes several studies of induced (rather than spontaneous, as above) regeneration with adult mammals using the collagen scaffold with regenerative activity (DRT) that was referred to in preceding sections. This scaffold has been shown to dramatically delay the onset of skin wound contraction or to cancel contraction, while inducing regeneration in the guinea pig, rat, rabbit, swine, and (with limited quantitative data) in the human; and in three organs, i.e., skin, peripheral nerves and the rabbit conjunctiva (review in (55)). Support for the role of contraction blocking in induction of regeneration was obtained using a series of closely matched controls for DRT (collagen scaffold library) with rodent models. (8) Some members of this library were active regeneratively but most were inactive to different degrees. (5) In one such library the members were identical in chemical structure but differed in average pore size, a determinant of the specific surface on the scaffold. With skin wounds in rodents, use of the library showed that contraction was delayed most strongly, while regeneration occurred most prominently, when the scaffold pore size was in the range 20–125 μm; the contraction delay time dropped rapidly while regeneration was observed outside this range of the pore size. (8) The data essentially showed a coincidence of strong contraction delay, or blocking, and regeneration along the several members of the scaffold library.

A different collagen scaffold library was used in studies of peripheral nerve wounds in the sciatic nerve of the rat. Here, the particular collagen library used comprised members that were identical in pore size but differed in crosslink density; the latter property correlated positively with the degradation half-life. (9,36,56) It was observed that scaffold library members that induced formation of thicker capsules of contractile cells around the nerve stumps were associated with a decreased diameter of neural tissue and decreased number of myelinated axons, both clear signs of a lower quality of nerve regeneration (Fig. 5 *right*). The number of A-fibers measured in the regenerate in the same study also showed a significant drop with increase in capsule thickness. (9) As expected, the number of myelinated axons per cross section decreased monotonically along the series with decrease in neural tissue diameter. (9) In a characteristic example associated with the data of Fig. 5 *left*, the diameter of the regenerated neural tissue decreased from about 0.59 mm to 0.28 mm, and the number of myelinated fibers decreased from about 7000 to 800 per cross

section of neural tissue, while the corresponding thickness of the capsule increased from about 22 μm to 98 μm. Use of tubes fabricated from contraction-blocking DRT maximized the diameter along the scaffold series and simultaneously led to minimization of capsule thickness (see locations marked DRT in Fig. 5, *left, right*). A photographic record from this study documents in detail the inverse relationship between the thickness of the contractile capsule and the corresponding quality of nerve regeneration. (9) We suggest that the data in Fig. 5 amount to direct quantitative evidence that contraction and regeneration are antagonistically related.

A third organ in the adult mammal that has shown an inverse relation between contraction and induction of regeneration is the conjunctiva in the rabbit. (57) Though preliminary, the conjunctiva results with the rabbit model are consistent with observations obtained with skin and peripheral nerve wounds.

Although there is direct evidence from studies of spontaneous healing as well as studies of induced healing with DRT, showing that blocking of wound contraction coincides with induced regeneration, there is also evidence showing that such an arguably necessary condition is, nevertheless, not sufficient to induce regeneration. This conclusion comes out of several studies of impaired healing of skin wounds in animal models, i.e., wounds deliberately treated in a variety of ways that induce healing under pathological or artificial conditions that prevent wound contraction. Examples are wounds in animals treated with steroids; (58–62) wounds in genetically diabetic animals (63,64) and in genetically obese animals (64); and splinted wounds that prevent contraction. (65) These skin wound models showed greatly delayed or cancelled contraction yet there was no evidence of regeneration in any of these studies of impaired healing. In these impaired wounds, blocking of contraction did not suffice to induce regeneration.

The simplest explanation of the diverse evidence summarized above, obtained with a large variety of species and anatomical sites, is that contraction blocking in skin wounds and peripheral nerve wounds appears to be necessary, but does not suffice, to induce regeneration. However, there is inadequate information to justify a claim of causality between contraction blocking and induction of regeneration.

Surface biology of wound contraction blocking by a collagen scaffold with highly specific structure

The highly porous structure of DRT, studied for example by scanning electron microscopy, reveals the extensive surface of this scaffold but not the active sites (ligands) for cell adhesion on the scaffold surface. These ligands are required for MFB integrin binding which appears to control a critical change in MFB phenotype.

A spontaneously healing skin wound which normally contracts vigorously undergoes a dramatic transformation when grafted with DRT. Use of DRT leads to cancellation or significant delay of wound contraction. (8,10) Both in skin and peripheral nerve wounds, the originally dense cell assemblies, comprising myofibroblasts (MFB) with high alignment, change into a configuration which has an MFB density reduced to 20% of that in the

ungrafted wound (see (6)), with extensive dispersion of the assembled cells and almost complete randomization of long cell axes (Fig. 7 top, skin wounds; Fig. 7 bottom, peripheral nerve wounds). These changes correspond to a profound change in cell phenotype and appear to account for the observed cancellation of the macroscopic contraction force, estimated at 0.1 N in a rodent model of a dorsal skin wound. (66) We summarize below the molecular events which appear to explain these changes in cell phenotype and account for the contraction-blocking activity of DRT at the molecular scale.

The observed reduction in myofibroblast density in DRT-treated wounds can be explained most simply by the observed downregulation in concentration level of transforming growth factor beta1 (TGFβ1), the key cytokine required for myofibroblast differentiation. (19) In the presence of the DRT scaffold-tube, the concentration of TGFβ1 in the peripheral nerve wound was reduced to 72% relative to the regeneratively inactive control tube (silicone tube); and alpha smooth muscle actin, a myofibroblast marker, was reduced to a level as low as 13% of the concentration level observed with the inactive collagen control. (9) The origin of the observed downregulation in TGFβ1 concentration in the presence of DRT is not clearly understood at present; it could hypothetically result from the great affinity with which TGFβ1 has been shown to bind nonspecifically on the DRT surface, to an extent of about 7 μg TGFβ1/mg DRT, (67) and the resulting likelihood of reduction in activity of the bound (relative to the free) cytokine. An alternative explanation of the significant downregulation in MFB density in the presence of the phenotype-changing DRT can be couched in terms of the loss in tension, a known prerequisite for MFB differentiation (19). Other explanations have been also proposed. (5)

Dispersion of cell assemblies and disorientation of long axes of cells in the presence of DRT is explained most simply by inhibition of MFB-MFB binding and facilitation instead of MFB-DRT binding. How does this happen at the molecular scale?

A novel methodology based on 3D two-photon microscopy has been described for quantifying *in situ* the density of ligands for adhesion receptors (collagen binding integrins) on the surface of a 3D matrix. (37) This method has been used to measure the adhesion ligand density for the two major collagen-binding integrins ($\alpha_1\beta_1$, $\alpha_2\beta_1$) in two kinds of porous collagen scaffolds that differed greatly in regenerative activity in a peripheral nerve regeneration study. (9) The ligands for these two integrins were identified as GFOGER and GLOGEN, Fig. 8.

In this study, two scaffolds with sharply differing regenerative activity (referred to below as “active” and “inactive”) were members of the same collagen library and were nearly identical in structure; they differed, however, in their crosslink density which is known to control the degradation half-life of the two scaffolds to different levels (higher crosslink density and longer half-life observed with the inactive scaffold). Use of the active scaffold resulted in peripheral nerve regeneration of a significantly higher quality than that observed with the inactive scaffold. The ligand concentration on the surface of the active scaffold was much higher than that on the inactive one, Fig. 8. (37) Although preliminary, the available evidence suggests the possibility that adhesive cell-matrix binding, enabled by the sufficiently dense presence of integrin-binding ligands on the surface of the active scaffold,

can be used to explain the observed inhibition of MFB-MFB binding (shown as dispersion of MFB assemblies; see Fig. 2 *bottom*, 3A *right* and 3B *right*) and corresponding facilitation of MFB-DRT binding.

Use of collagen libraries has shown that at least three structural features in DRT required adjustment to levels that were critical for biological activity. Maximum regenerative activity with simultaneous maximum contraction blocking were observed when the pore size for collagen scaffolds in one library was varied in the range 20–125 μm (8) while the optimal degradation half-life for this scaffold was maintained fixed at 14 ± 7 d.(9,36) Insufficient data are available to identify optimal values for ligand densities for integrins $\alpha_1\beta_1$ and $\alpha_2\beta_1$. The limited evidence suggests a threshold for regenerative activity, corresponding to a minimal level of ligand density for the two integrins, that exceeds 200 μM $\alpha_1\beta_1$ or $\alpha_2\beta_1$ μM ligands. (37) Substantial departure from optimal levels with any of these three structural features, namely, pore size, degradation half-life and ligand density, deactivates DRT almost completely and yields scaffolds that have little or no regenerative activity.

An analysis of these optimal values provides an explanation for their mechanistic importance during contraction blocking which precedes the regeneration process. The lower level of scaffold pore size appears to be necessary to provide minimal space for contractile cell migration inside the scaffold where cell binding takes place. An upper limit in pore size is required to provide sufficient specific surface on the scaffold for binding of all (or most) of the contractile cells present in the wound grafted with DRT (the specific surface of a porous material is known to decrease regularly with average pore size). The limiting values for scaffold degradation half-life appear to be related to the duration of the myofibroblast life cycle. Myofibroblasts appear in a full-thickness guinea pig skin wound within about 1 week following injury and disappear in about 3–4 weeks (due to apoptosis). A lower limit for scaffold degradation half-life is required in order to ensure that a sufficient number of myofibroblasts has become differentiated in the wound and can make phenotype-changing adhesive contact with the scaffold surface before the latter is degraded. The upper limit for scaffold half-life probably marks the time for myofibroblast apoptosis (about 30 days in the guinea pig model used) beyond which effective contact with the scaffold surface is apparently precluded. The degradation half-life limits on scaffold structure noted here are therefore accounted for by the requirement for an adequate number of contractile cells to bind on a scaffold surface endowed with sufficient ligands, during a period which lasts just enough to provide for contact between cells and the scaffold surface.

We have argued above that regeneration can be induced by the apparently simple device of control of the wound healing process in skin and peripheral nerves. The desired level of control is achieved by use of a biologically active surface, a collagen scaffold with structure optimized for maximal regenerative activity, which dramatically modifies the contractile phenotype of myofibroblasts, leading to inhibition of wound contraction that appears to be required for induction of regeneration.

Discussion

According to the deformation field theory of scar formation presented above, scar formation in injured skin or peripheral nerves requires the presence of the mechanical field of the contracting wound that aligns collagen-synthesizing cells, and eventually aligns the resulting collagen fibers as well, along the direction of the major tissue deformation axis. The theory explains well the available morphological data that characterize the relation between major deformations and scar morphology both in contracting skin and peripheral nerve wounds.

The evidence shows that scar formation appears to be a process secondary (derivative) to wound contraction. Regeneration of skin and peripheral nerves in adults appears, therefore, to be primarily thwarted by contraction, not by scar formation. This distinction is of critical importance in devising new regenerative approaches. However, no data are presented in this review on the injured central, rather than peripheral, nervous system and it is not possible to assess the effect of scar formation on regeneration in this system, a hypothesis proposed elsewhere. (e.g. 2–4)

The importance of mechanical fields in contraction of wounds in other organs has been proposed in the literature in terms of alternative theoretical treatments of scar formation. For example, in a recent study of healing of the myocardial infarct in the rat heart the authors concluded that the mechanical field determines the arrangement of collagen fiber in the healed infarct. (68) A mathematical biomechanical model was recently developed to simulate wound contraction and scar formation. (69).

The second main conclusion reached in this article originates in evidence from diverse species and shows that, simply put, contraction and regeneration do not appear to occur together during healing of skin wounds and peripheral nerve wounds. This conclusion is supported by a set of independent observations of spontaneous regeneration (scarless healing) without contraction, or very limited contraction, of skin wounds in a developing amphibian (tadpole), two animal models that are well-known in studies of regeneration (perforated rabbit ear, skin wounds in the axolotl) and in a specific anatomic site of the swine and mouse (oral mucosa). Studies of induced regeneration using DRT and related collagen scaffold libraries provide a complementary set of data, showing a direct association between blocking of contraction and absence of scar, on one hand, with induced regeneration of the respective organs, on the other. In particular, peripheral nerve studies with DRT tubes using a library of closely matched collagen scaffolds showed a progressive increase in quality of regeneration with increased evidence of blocking of contraction around the stumps, (9) arguably similar to a quantitative dose-response relation between these two variables (Fig. 5). We note that the evidence showing that contraction and regeneration oppose each other originates in diverse and independent sources. Even though no causal relation is proposed here, the conclusion of such an antagonistic relation must be taken into account in future studies of spontaneous or induced regeneration.

A hypothesis that contraction is an antagonist to regeneration can be tested by studies with the mammalian fetus, admittedly an experimentally challenging configuration. It is known that scarless healing occurs prior to the ontogenetic transition that is observed between early

and late gestation; after the transition, wounds close with scar. (70–72) The hypothesis described here makes the testable prediction that the period of scarless healing during fetal gestation coincides with absence of wound contraction; and that, after the transition, healing with scar coincides with the incidence of wound contraction.

The collagen scaffold, DRT, that blocks wound contraction and induces regeneration requires very careful adjustment of its structural features to levels that optimize cell-scaffold adhesion for almost all contractile cells in a wound, an apparent prerequisite for its activity. The data with the scaffold libraries (8,9,36) make it clear that a casually structured collagen scaffold that does not incorporate the three critical structural features identified above would almost certainly lack regenerative activity. This conclusion explains why so many collagen implants reported in the literature have failed to induce regeneration. Furthermore, the requirement for ligands on the surface of DRT discourages consideration of scaffolds based on synthetic polymers in efforts to induce regeneration. It is clear from the data obtained by two-photon microscopy (5,37) that the surface biology of the cell-scaffold interaction plays a key role in the observed regenerative activity of DRT, Fig. 8. This finding extends greatly the concept of biological activity from its usual emphasis on soluble proteins, soluble enzymes, etc., typically present in dilute aqueous solution, to an insoluble, solid-like surface. A surface is apparently required in order to bring about a phenotype change of major importance.

Two sets of data show that regeneration of skin and peripheral nerves share a common mechanism. First, in both organs the spontaneous (DRT-free) wound healing process is driven by a contractile mechanical field that establishes the collagen fiber architecture in skin scar and neural scar. The major configurational difference between the healing processes in the two organs is the topography of the respective organ (planar in skin, cylindrical in PN) rather than other kinds of differences between the two organs. Second, in both organs, grafting of wounds with DRT induces the same mechanistic change in myofibroblast phenotype (reduction in MFB density, dispersion of MFB assemblies, loss of alignment of MFB axes) that is associated with blocking of contraction and initiating the process of regeneration. This conclusion encourages extension of this regenerative methodology to other organs as well.

In summary, the evidence presented here supports the two conclusions that scar formation in skin wounds and PN wounds is a process secondary (derivative) to wound contraction; and that contraction and regeneration are antagonistically related to each other in both of these organs. These conclusions converge to identify the importance of wound contraction as the central process during spontaneous wound healing as well as during induced regeneration. A relatively simple modification of the normal healing process, based on use of the contraction-blocking DRT scaffold, provides a reliable route towards regeneration of skin and peripheral nerves. In addition, elucidation of the molecular mechanism by which regeneration is induced provides a useful mechanistic basis for future development of regenerative science and medicine.

Acknowledgments

IVY was partly supported by grant RO1 NS051320 from the National Institutes of Health. DST acknowledges support from the People Programme (Marie Curie Actions) of the European Union's Horizon 2020 under REA grant agreement DLV-658850. PTCS acknowledges support from National Institutes of Health 5-P41-EB015871-28, Singapore-MIT Alliance for Science and Technology, and Hamamatsu Photonics Corp.

References

1. Yates CC, Hebda P, Wells A. Skin wound healing and scarring: fetal wounds and regenerative restitution. Birth Defects Res C Embryo Today. 2012; 96:325–333. [PubMed: 24203921]
2. Kiernan JA. Hypotheses concerned with axonal regeneration in the mammalian nervous system. Biol Rev Camb Philos Soc. 1979; 54(2):155–97. [PubMed: 383167]
3. Esmaeili M, Berry M, Logan A, Ahmed Z. Decorin treatment of spinal cord injury. Neural Regen Res. 2014; 9(18):1653–6. [PubMed: 25374584]
4. Vogelaar CF, König B, Krafft S, Estrada V, Brazda N, Ziegler B, et al. Pharmacological Suppression of CNS Scarring by Deferoxamine Reduces Lesion Volume and Increases Regeneration in an In Vitro Model for Astroglial-Fibrotic Scarring and in Rat Spinal Cord Injury In Vivo. PLoS One. 2015; 10(7):e0134371. [PubMed: 26222542]
5. Yannas IV, Tzeranis DS, So PT. Surface biology of collagen scaffold explains blocking of wound contraction and regeneration of skin and peripheral nerves. Biomed Mater. 2015; 11(1):014106. [PubMed: 26694657]
6. Murphy GF, Orgill DP, Yannas IV. Partial dermal regeneration is induced by biodegradable collagen-glycosaminoglycan grafts. Lab Invest. 1990; 62:305–313. [PubMed: 2314050]
7. Yannas, IV. Use of artificial skin in wound management. In: Dineen, P., editor. The Surgical Wound. Philadelphia: Lea & Febiger; 1981. p. 171-190.
8. Yannas IV, Lee E, Orgill DP, Skrabut EM, Murphy GF. Synthesis and characterization of a model extracellular matrix which induces partial regeneration of adult mammalian skin. Proc Natl Acad Sci USA. 1989; 86:933–937. [PubMed: 2915988]
9. Soller EC, Tzeranis DS, Miu K, So PT, Yannas IV. Common features of optimal collagen scaffolds that disrupt wound contraction and enhance regeneration both in peripheral nerves and in skin. Biomaterials. 2012; 33:4783–91. [PubMed: 22483241]
10. Yannas IV, Burke JF, Orgill DP, Skrabut EM. Wound tissue can utilize a polymeric template to synthesize a functional extension of skin. Science. 1982; 215:174–176. [PubMed: 7031899]
11. Burke JF, Yannas IV, Quinby WC Jr, Bondoc CC, Jung WK. Successful use of a physiologically acceptable artificial skin in the treatment of extensive burn injury. Ann Surg. 1981; 194:413–428. [PubMed: 6792993]
12. Gabbiani G, Ryan GB, Majno G. Presence of modified fibroblasts in granulation tissue and possible role in wound contraction. Experientia. 1971; 27:549–550. [PubMed: 5132594]
13. Rudoph R. Location of the force of wound contraction. Surg Gynecol Obst. 1979; 148:547–551. [PubMed: 432768]
14. Rudolph, R., Van de Berg, J., Ehrlich, P. Wound contraction and scar contracture. In: Cohen, IK.Diegelmann, RF., Lindblad, WJ., editors. Wound Healing. Philadelphia: W.B. Saunders; 1992.
15. Gabbiani G. Evolution and clinical implications of the myofibroblast concept. Cardiov Res. 1998; 38:545–548.
16. Daimon E, Shibukawa Y, Wada Y. Calponin 3 regulates stress fiber formation in dermal fibroblasts during wound healing. Arch Dermatol Res. 2013; 305:571–84. [PubMed: 23545751]
17. Tomasek JJ, Haaksma CJ, Schwartz RJ, Howard EW. Whole animal knockout of smooth muscle alpha-actin does not alter excisional wound healing or the fibroblast-to-myofibroblast transition. Wound Repair Regen. 2013; 21(1):166–76. [PubMed: 23253249]
18. Hinz B, Phan SH, Thannickal VJ, Prunotto M, Desmoulière A, Varga J, et al. Recent developments in myofibroblast biology: paradigms for connective tissue remodeling. Am J Pathol. 2012; 180:1340–55. [PubMed: 22387320]

19. Desmoulière A, Chaponnier C, Gabbiani G. Tissue repair, contraction, and the myofibroblast. Wound Repair Regen. 2005; 13:7–12. [PubMed: 15659031]
20. Desmoulière A, Redard M, Darby I, Gabbiani G. Apoptosis mediates the decrease in cellularity during the transition between granulation tissue and scar. Am J Pathol. 1995; 146:56–66. [PubMed: 7856739]
21. van Beurden HE, Von den Hoff JW, Torensma R, Maltha JC, Kuijpers-Jagtman AM. Myofibroblasts in palatal wound healing: prospects for the reduction of wound contraction after cleft palate repair. J Dent Res. 2005; 84:871–80. [PubMed: 16183784]
22. Spector M. Musculoskeletal connective tissue cells with muscle: Expression of muscle actin in and contraction of fibroblasts, chondrocytes, and osteoblasts. Wound Repair Regen. 2001; 9:11–18. [PubMed: 11350635]
23. Hebda PA, Collins MA, Tharp MD. Mast cell and myofibroblast in wound healing. Dermatol Clin. 1993; 11(4):685–96. [PubMed: 8222352]
24. Ehrlich HP, Keefer KA, Myers RL, Passaniti A. Vanadate and the absence of myofibroblasts in wound contraction. Arch Surg. 1999; 134(5):494–501. [PubMed: 10323421]
25. Ehrlich HP, Allison GM, Leggett M. The myofibroblast, cadherin, alpha smooth muscle actin and the collagen effect. Cell Biochem Funct. 2006; 24:63–70. [PubMed: 15584087]
26. Ehrlich HP, Hunt TK. Collagen Organization Critical Role in Wound Contraction. Adv Wound Care (New Rochelle). 2012; 1(1):3–9. [PubMed: 24527271]
27. Ehrlich HP, Moyer KE. Cell-populated collagen lattice contraction model for the investigation of fibroblast collagen interactions. Methods Mol Biol. 2013; 1037:45–58. [PubMed: 24029929]
28. Crandall, SH., Dahl, NC., Lardner, TJ. An Introduction to the Mechanics of Solids. New York: McGraw-Hill; 1972. p. 209
29. Birk, DE., Trelstad, RL. Fibroblasts compartmentalize the extracellular space to regulate and facilitate collagen fibril, bundle, and macro-aggregate formation. In: Reddi, AH., editor. Extracellular Matrix: Structure and Function. New York: Alan R. Liss; 1985.
30. Ferdman AG, Yannas IV. Scattering of light from histologic sections: A new method for the analysis of connective tissue. J Invest Dermatol. 1993; 100:710–716. [PubMed: 7684057]
31. Hunter JAA, Finlay JB. Scanning electron microscopy of normal scar tissue and keloids. Br J Plast Surg. 1976; 63:826–830.
32. Knapp TR, Daniels JR, Kaplan EN. Pathologic scar formation. Am J Pathol. 1977; 80:47–63.
33. Van Zuijlen PP, de Vries HJ, Lamme EN, Coppens JE, van Marle J, Kreis RW, Middelkoop E. Morphometry of dermal collagen orientation by Fourier analysis is superior to multi-observer assessment. J Pathol. 2002; 198(3):284–91. [PubMed: 12375260]
34. Grant CA, Twigg PC, Tobin DJ. Static and dynamic nanomechanical properties of human skin tissue using atomic force microscopy: effect of scarring in the upper dermis. Acta Biomater. 2012; 8(11):4123–9. [PubMed: 22771457]
35. Chamberlain LJ, Yannas IV, Hsu HP, Spector M. Connective tissue response to tubular implants for peripheral nerve regeneration: The role of myofibroblasts. J Comp Neurol. 2000; 417:415–430. [PubMed: 10701864]
36. Harley BA, Spilker MH, Wu JW, Asano K, Hsu HP, Spector M, Yannas IV. Optimal degradation rate for collagen chambers used for regeneration of peripheral nerves over long gaps. Cells Tissues Organs. 2004; 176:153–65. [PubMed: 14745243]
37. Tzeranis DS, Soller EC, Buydash MC, So PT, Yannas IV. In Situ Quantification of Surface Chemistry in Porous Collagen Biomaterials. Ann Biomed Eng. 2016; 44(3):803–15. [PubMed: 26369635]
38. Yannas IV, Zhang M, Spilker MH. Standardized criterion to analyze and directly compare various materials and models for peripheral nerve regeneration. J Biomater Sci Polym Ed. 2007; 18:943–66. [PubMed: 17705992]
39. Yannas IV, Colt J, Wai YC. Wound contraction and scar synthesis during development of the amphibian Rana catesbeiana. Wound Rep Reg. 1996; 4:31–41.
40. Mustoe TA, Pierce GF, Morishima C, Deuel TF. Growth-factor induced acceleration of tissue repair through direct and inductive activities in a rabbit dermal ulcer model. J Clin Invest. 1991; 87:694–703. [PubMed: 1991853]

41. Joseph J, Dyson M. Tissue replacement in the rabbit's ear. Brit J Surg. 1966; 53:372–380. [PubMed: 5931030]
42. Goss RJ. Prospects for regeneration in man. Clin Orth. 1980; 151:270–282.
43. Goss, RJ. Regeneration versus repair. In: Cohen, IK.Diegelmann, RF., Lindblad, WJ., editors. Wound Healing. Philadelphia: W. B. Saunders; 1992.
44. Goss RJ, Grimes LN. Tissue interactions in the regeneration of rabbit ear holes. Am Zool. 1972; 12:151–157.
45. Goss RJ, Grimes LN. Epidermal downgrowths in regenerating rabbit ear holes. J Morphol. 1975; 146:533–542. [PubMed: 1171254]
46. Kennedy DF, Cliff WJ. A systematic study of wound contraction in mammalian skin. Pathol. 1979; 11:207–222.
47. Schrementi ME, Ferreira AM, Zender C, DiPietro LA. Site-specific production of TGF-beta in oral mucosal and cutaneous wounds. Wound Repair Regen. 2008; 16(1):80–6. [PubMed: 18086295]
48. Mak K, Manji A, Gallant-Behm C, Wiebe C, Hart DA, Larjava H, Häkkinen L. Scarless healing of oral mucosa is characterized by faster resolution of inflammation and control of myofibroblast action compared to skin wounds in the red Duroc pig model. J Dermatol Sci. 2009; 56(3):168–80. [PubMed: 19854029]
49. Wong JW, Gallant-Behm C, Wiebe C, Mak K, Hart DA, Larjava H, Häkkinen L. Wound healing in oral mucosa results in reduced scar formation as compared with skin: evidence from the red Duroc pig model and humans. Wound Repair Regen. 2009; 17(5):717–29. [PubMed: 19769724]
50. Larjava H, Wiebe C, Gallant-Behm C, Hart DA, Heino J, Häkkinen L. Exploring scarless healing of oral soft tissues. J Can Dent Assoc. 2011; 77:b18. [PubMed: 21366956]
51. Glim JE, van Egmond M, Niessen FB, Everts V, Beelen RH. Detrimental dermal wound healing: what can we learn from the oral mucosa? Wound Repair Regen. 2013; 21(5):648–60. [PubMed: 23927738]
52. Lévesque M, Villiard E, Roy S. Skin wound healing in axolotls: a scarless process. J Exp Zool B Mol Dev Evol. 2010; 314(8):684–97. [PubMed: 20718005]
53. Seifert AW, Monaghan JR, Voss SR, Maden M. Skin regeneration in adult axolotls: a blueprint for scar-free healing in vertebrates. PLoS One. 2012; 7(4):e32875. [PubMed: 22485136]
54. Lévesque M, Gatien S, Finnson K, Desmeules S, Villiard E, Pilote M, et al. Transforming growth factor: beta signaling is essential for limb regeneration in axolotls. PLoS One. 2007; 2(11):e1227. [PubMed: 18043735]
55. Yannas, IV. Tissue and Organ Regeneration in Adults. Extension of the paradigm to several organs. 2. New York: Springer; 2015.
56. Yannas IV, Burke JF, Huang C, Gordon PL. Correlation of in vivo collagen degradation rate with in vitro measurements. J Biomed Mater Res. 1975; 9:623–628. [PubMed: 171271]
57. Hsu WC, Spilker MH, Yannas IV, Rubin PAD. Inhibition of conjunctival scarring and contraction by a porous collagen-GAG implant. Invest Ophthalmol Vis Sci. 2000; 41:2404–2411. [PubMed: 10937547]
58. Billingham RE, Russell PS. Studies on wound healing, with special reference to the phenomenon of contracture in experimental wounds in rabbits' skin. Ann Surg. 1956; 144:961–981. [PubMed: 13373285]
59. Cuthbertson AM. Contraction of full thickness skin wounds in the rat. Surg Gynec Obstet. 1959; 108:421–432. [PubMed: 13635261]
60. McGrath MH. The effect of prostaglandin inhibitors on wound contraction and the myofibroblast. Plast Reconstr Surg. 1982; 69:71–83.
61. Fiddes JC, Hebda PA, Hayward P, Robson MC, Abraham JA, Klingbeil CK. Preclinical wound-healing studies with recombinant human basic fibroblast growth factor. Ann NY Acad Sci. 1991; 638:316–328. [PubMed: 1785809]
62. Hayward P, Hokanson J, Heggers J, Fiddes J, Klingbeil C. Fibroblast growth factor reverses the bacterial retardation of wound contraction. Am J Surg. 1992; 163:288–293. [PubMed: 1539760]
63. Greenhalgh DG, Sprugel KH, Murray MJ, Ross R. PDGF and FGF stimulate wound healing in the genetically diabetic mouse. Am J Pathol. 1990; 136:1235–1246. [PubMed: 2356856]

64. Klingbeil, CK., Cesar, LB., Fiddes, JC. Basic fibroblast growth factor accelerated tissue repair in models of impaired wound healing. In: Barbul, A.Caldwell, M.Eaglstein, W.Hunt, T.Marshall, D.Pines, E., Skover, G., editors. Clinical and Experimental Approaches to Dermal and Epidermal Repair: Normal and Chronic Wounds. New York: Alan R. Liss; 1991.

65. Hinz B, Mastrangelo D, Iselin CE, Chaponnier C, Gabbiani G. Mechanical tension controls granulation tissue contractile activity and myofibroblast differentiation. Am J Pathol. 2001; 159:1009–1020. [PubMed: 11549593]

66. Higton DLR, James DW. The force of contraction of full-thickness wounds of rabbit skin. Brit J Surg. 1964; 51:462–466. [PubMed: 14171056]

67. Thies, S. Unpublished data on the nonspecific binding of TGFb1 on the DRT scaffold. 2010.

68. Fomovsky GM, Rouillard AD, Holmes JW. Regional mechanics determine collagen fiber structure in healing myocardial infarcts. J Mol Cell Cardiol. 2012; 52(5):1083–90. [PubMed: 22418281]

69. Yang L, Witten TM, Pidaparti RM. A biomechanical model of wound contraction and scar formation. J Theor Biol. 2013; 332:228–48. [PubMed: 23563057]

70. Estes JM, Vande Berg JS, Adzick NS, MacGillivray TE, Desmoulière A, Gabbiani G. Phenotype and functional features of myofibroblasts in sheep fetal wounds. Differentiation (Berl). 1994; 56:173–181.

71. Beanes SR, Hu FY, Soo C, Dang CM, Urata M, Ting K, et al. Confocal microscopic analysis of scarless repair in the fetal rat: defining the transition. Plast Reconstr Surg. 2002; 109:160–70. [PubMed: 11786808]

72. Soo C, Beans SR, Hu FY, Zhang X, Dang C, Chang G, et al. Ontogenetic transition in fetal wound transforming growth factor-β regulation correlates with collagen organization. Am J Path. 2003; 163:2459–2476. [PubMed: 14633618]

73. Troxel, K. PhD thesis. Massachusetts Institute of Technology; Cambridge, MA: 1994. Delay of skin wound contraction by porous collagen-GAG matrices.

74. Tzeranis, DS. PhD thesis. Massachusetts Institute of Technology; Cambridge, MA: 2013. Imaging studies of peripheral nerve regeneration induced by porous collagen biomaterials.

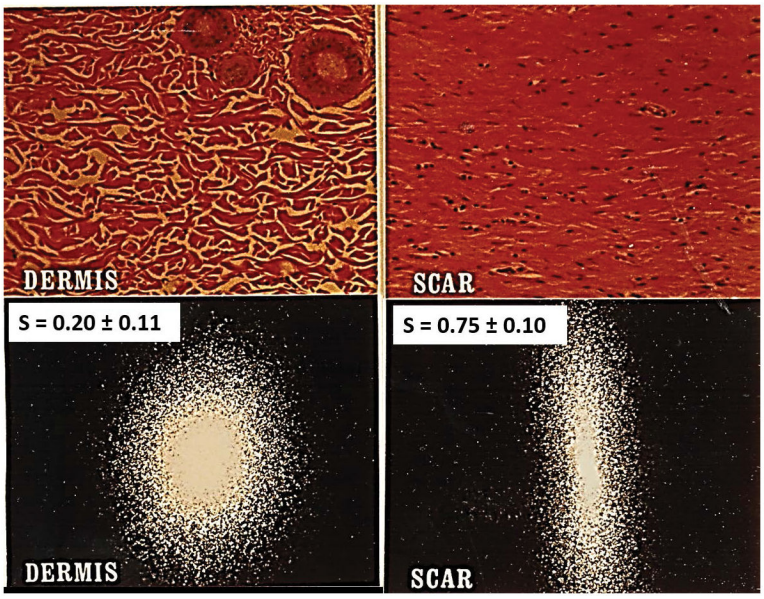

Figure 1.

Quantitative distinction between scar and physiologic dermis in guinea pig skin using laser light scattering from histological tissue sections. Representative scattering patterns for dermis and scar can be analyzed to compute the orientation index, S, which varies from 0 (perfectly random alignment) to 1 (perfect alignment). *Top*: Histologic views from the reticular region of normal dermis (*left*) and from scar (*right*). *Bottom left*: Laser scattering patterns from dermis, showing S = 0.20 ± 0.11, indicative of a largely random orientation pattern with a small component of alignment (in the epidermal plane). *Bottom right*: Scar shows S = 0.75 ± 0.10, indicating high, but not perfect, orientation. (Adapted from (30)).

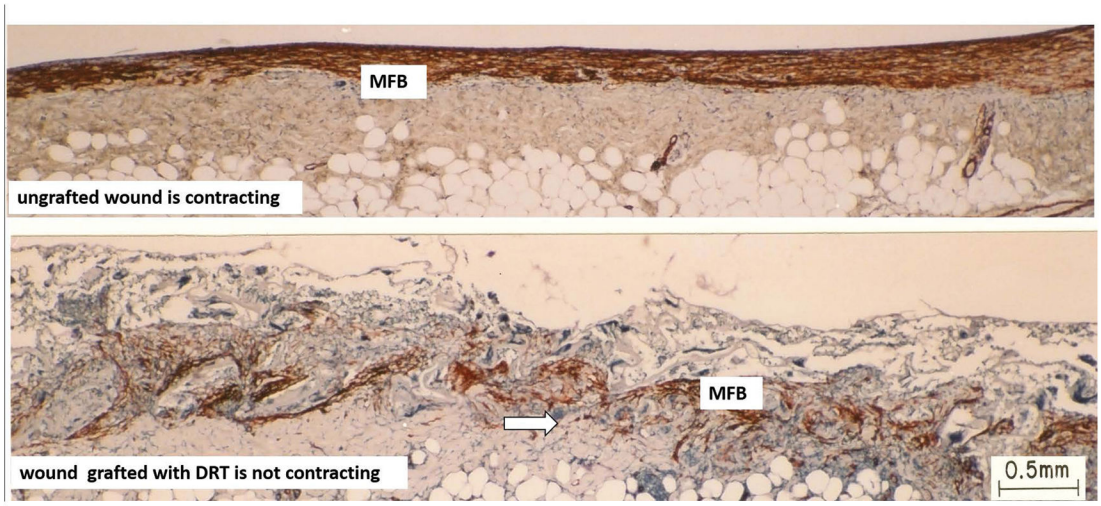

Figure 2. Skin wounds

Sharply contrasting behavior during healing of two full-thickness skin wounds in the guinea pig. Histology sections were stained with antibody to α-smooth muscle actin. *Top*: Ungrafted wound is contracting vigorously on day 10. Dense assemblies of highly oriented contractile cells (myofibroblasts, MFB; *red brown*) populate the wound. *Bottom*: Wound grafted with a collagen scaffold, the dermis regeneration template (DRT), is not contracting on day 11. Grafting with DRT (*bottom*) resulted in significant reduction in MFB, dispersion of MFB assemblies and randomization of alignment of MFB axes. These changes describe a dramatic change in MFB phenotype and hypothetically account for the observed cancellation of the macroscopic contractile force in the wound. *Red brown*, MFB. *Arrows*: Scaffold struts. Scale bar: 0.5 mm. (adapted from (73)).

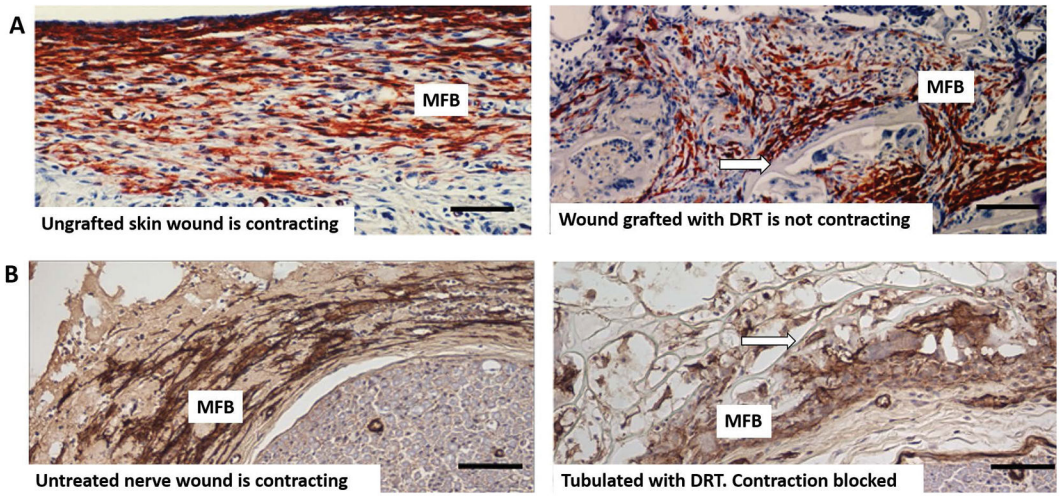

Figure 3.

A: Skin wounds. High magnification view of guinea pig skin wounds from Fig. 2, prepared by full-thickness excision, shows changes in myofibroblast phenotype following grafting with the dermis regeneration template (DRT). Immunohistochemical localization of α-SMA corresponds to the myofibroblast phenotype (MFB, *red brown*). *Left*: Untreated skin wound is contracting (10 days). MFB are dense, assembled closely and their long axes are oriented in the plane of the wound. *Right:* Skin wound grafted with DRT is not contracting (11 days). Compared to untreated wound (*left*), MFB show lower density, dispersed cell assemblies and lack of alignment of cell axes. *Arrow*: scaffold strut. Scale bars: 100 μm (adapted from (73)).

B: Peripheral nerve wounds. High magnification view of two peripheral nerve wounds observed at 14 days after complete transection of the rat sciatic nerve. Immunohistochemical localization of α-SMA (indicative of myofibroblast phenotype) in the contractile cell capsule surrounding the nerve stumps (MFB, *brown*). *Left*: Untreated (untubulated) wound. MFB are dense, assembled closely and their long axes are mostly oriented circumferentially around the neural tissue (*bottom right*). *Right*: Wound tubulated with DRT. Compared to untreated nerve (*left*), MFB show lower density, dispersed cell assemblies and lack of circumferential orientation of cell axes around the neural tissue (*bottom right*). (adapted from (9)). *Arrow*: scaffold strut. Scale bars: 100 μm

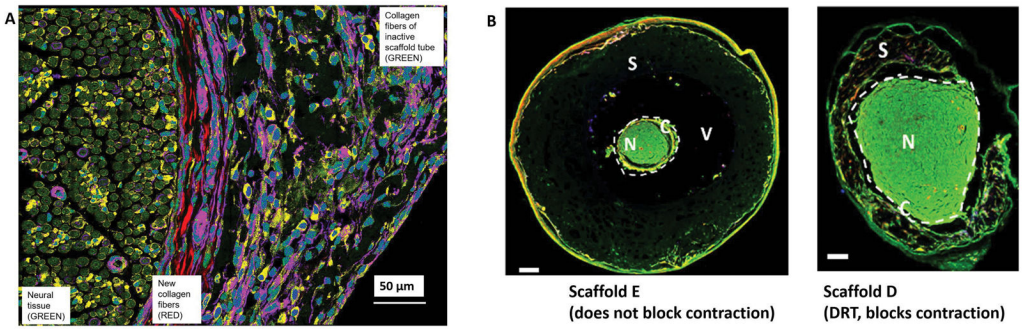

Figure 4.

A: Peripheral nerve wounds. Circumferential arrangement of collagen fibers around neural tissue during healing of the completely transected rat sciatic nerve. Observed by high resolution spectral multi-photon imaging. The transected nerve was tubulated with the regeneratively inactive scaffold A, member of a collagen scaffold library described in the text. The initial gap length was 15 mm. The nerve regenerate was observed at 9 weeks post injury and at 1.5 mm away from the proximal stump. The left section of the photo shows the newly-regenerated neural tissue (*green*); the central section shows newly synthesized collagen fibers surrounding the perimeter of neural tissue (*red*); the right section shows the semi degraded remnants of the porous inactive collagen scaffold (*purple-green*). Scale bar: 50 µm (adapted from (74)). **B:** Peripheral nerve wounds. Two nerve cross sections, illustrating the effect of two collagen scaffolds, members of a in internally controlled scaffold library, on the extent of contraction of the regenerating nerve diameter at 9 weeks. The rat sciatic nerve was completely transected and the initial gap length was 15 mm. The scaffold library comprised members that differed in degradation half-life (described in detail in Harley et al., 2004; Soller et al., 2012). *Left*: Tubulated with Scaffold E, with long degradation half-life, which did not interfere with normal contraction of the nerve diameter following transection. Neural tissue (*N*, *green*) shows a small diameter, is surrounded by a contractile cell capsule (C) and serum (*V*). The nerve does not make close contact with the largely undegraded scaffold (*S*). *Right*: Nerve was tubulated with Scaffold D, similar in structure to DRT, which blocks contraction of the nerve diameter. Scaffold D had a relatively short degradation half-life (see also text). *N*, Neural tissue (*N*, *green*) shows a large diameter and is surrounded by a contractile cell capsule (*C*). *S*, partly degraded scaffold. Fluorescent imaging. Scale bars: 200 µm. (adapted from (37)).

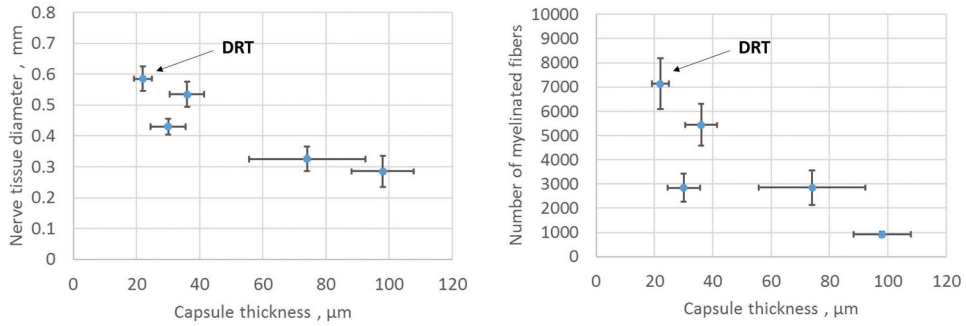

Figure 5. Peripheral nerve wounds

The quantitative effect of thickness of the contractile cell capsule (MFB capsule) on the properties of the regenerating nerve at 9 weeks post injury. The rat sciatic nerve was transected and the stumps were inserted inside five collagen tubes with closely matched but nonidentical scaffold structures, differing in half-life for degradation. The nerve stumps were originally separated by a gap length of 15 ± 1 mm. Data were obtained with the regenerated nerve that formed at the midpoint of the original stump separation. The contractile cell capsule stained positively for the myofibroblast phenotype and surrounded circumferentially the regenerating nerve, as illustrated in Fig. 3B (*left*) and Fig. 4A. *Left*: An inverse relationship was observed between the thickness of the contractile cell capsule and the diameter of the regenerating nerve. The nerve tissue diameter was estimated as the square root of the total myelinated area. *Right*: The number of myelinated axons decreased sharply with increase in thickness of the contractile cell capsule surrounding the regenerating rat sciatic nerve. *DRT*, indicates location of DRT (dermis regeneration template) scaffolds which were associated with maximum regenerative activity (adapted from (9)).

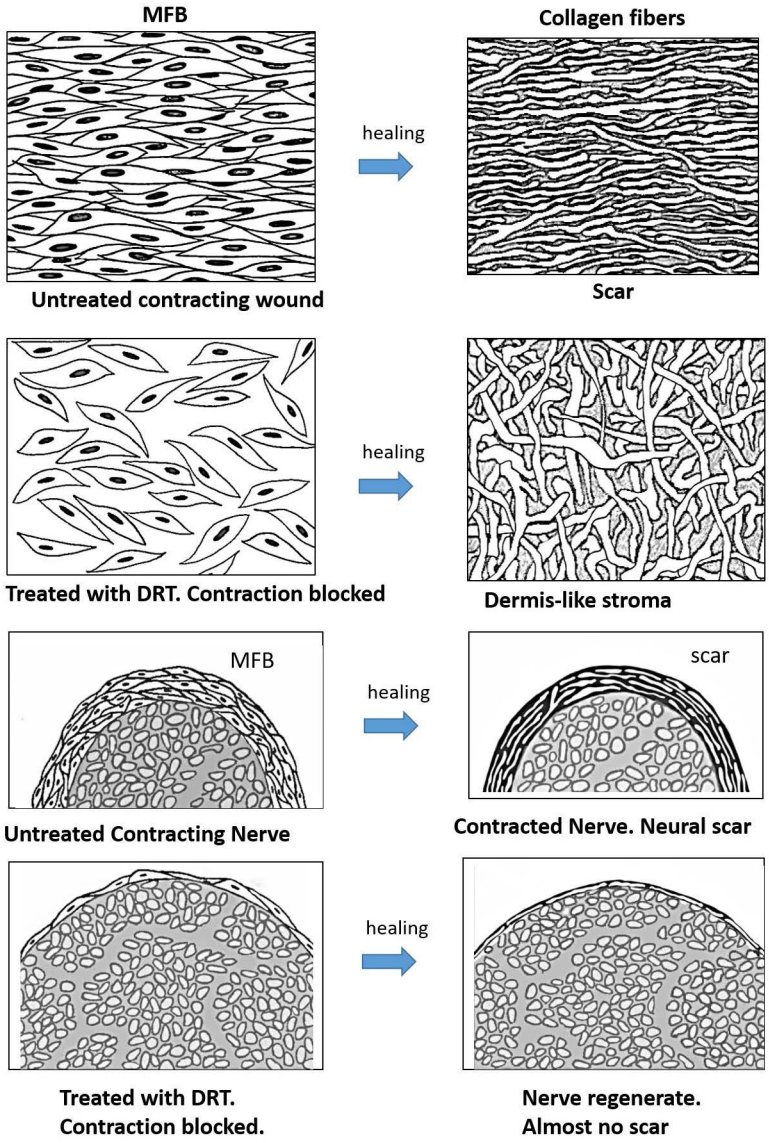

Figure 6.

Schematic illustration of the deformation theory of scar formation in full-thickness skin wounds and in a fully transected peripheral nerves. *Row 1:* wound untreated with the dermis regeneration template (DRT) contracts normally and heals with scar formation. A dense field of myofibroblasts (MFB), comprising cells that are closely assembled and highly aligned (based on data in Fig. 3A, *top left*), induces strong contraction and synthesizes collagen fibers that have the same high alignment as the long axes of cells, resulting in skin scar (based on data in Fig. 1 *right*). *Row 2*: in a skin wound treated (grafted) with DRT, the MFB density is attenuated, cell assembly is dispersed and alignment of cells is nearly random, leading to synthesis of collagen fibers that are randomly aligned, resembling the normal dermis (based on data in Fig. 3A, *top right*). *Row 3*: nerve untreated (untubulated) with DRT contracts normally in the presence of a thick myofibroblast (MFB) layer (based on data in Fig. 4B, *left*) and heals with formation of a thick layer of circumferential scar (see text for

documentation; also see Fig. 7 in (35)). The nerve diameter is relatively small, the myofibroblast layer surrounding the nerve is thick, and the resulting scar layer is also thick. *Row 4*: in a nerve tubulated with DRT scaffold contraction is blocked and the transected nerve heals with formation of a nearly normal nerve trunk (based on data in Fig. 4B, *right*). The nerve diameter is large, the myofibroblast layer surrounding it is very thin and the resulting scar layer is also very thin. Schematic myofibroblast layer thickness (capsule thickness) was based on data in Fig. 5; nerve diameters were based on photos in Figs. 4B and 5; neural scar layer thickness in untubulated and tubulated nerve trunks was based on photos in Fig. 7 of (35) (graphic by A. Maragh).

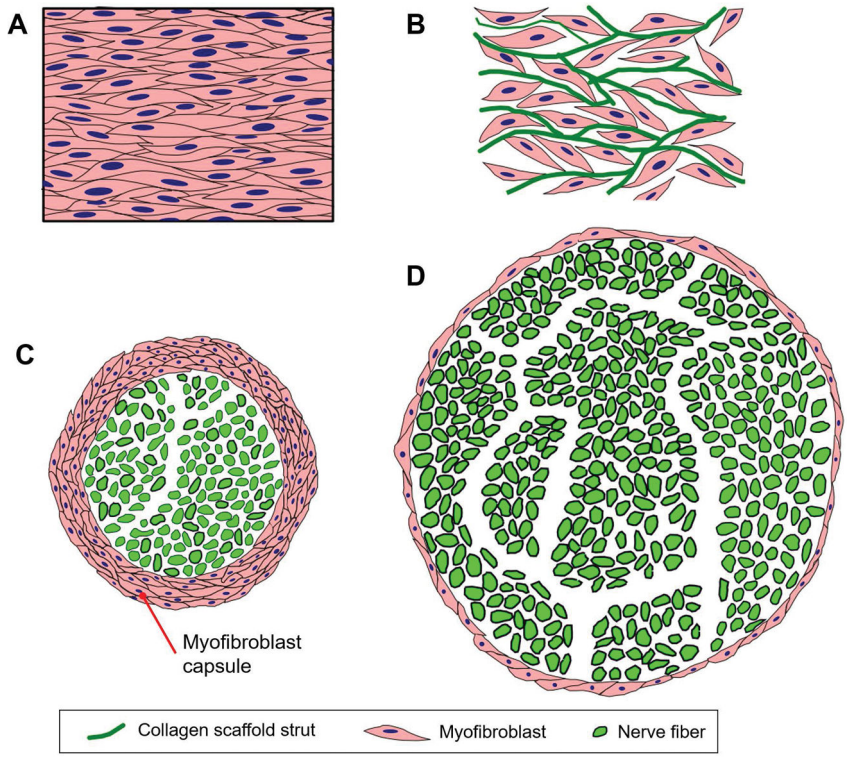

Figure 7.

Large-scale organized structures of contractile myofibroblasts (MFB) are the cellular origins of wound contraction and scar formation in skin and peripheral nerves. A: In ungrafted skin wounds, large numbers of MFB form a thick cellular capsule. The long axes of MFB are oriented parallel to the plane of the epidermis. Elementary forces applied by each MFB sum up to a significant resulting force that contracts the injury site. Collagen fibers synthesized by MFB are also oriented along the same direction, leading to scar synthesis. B: In skin wounds grafted with DRT, MFB migrate inside the scaffold, bind on its surface and become randomly oriented. The resulting macroscopic contraction force is much smaller compared to the ungrafted wound. C: In ungrafted transected peripheral nerves, large numbers of MFB form a thick cellular capsule in the outer surface of the nerve regenerate. These MFB are oriented circumferentially around the nerve perimeter, generating a “pressure cuff” effect that compresses the neural tissue along the radial direction. D: In transected peripheral nerves grafted with porous collagen conduits based on DRT, the MFB capsule is much thinner and the resulting neural tissue synthesized is much larger in mass and axon content.

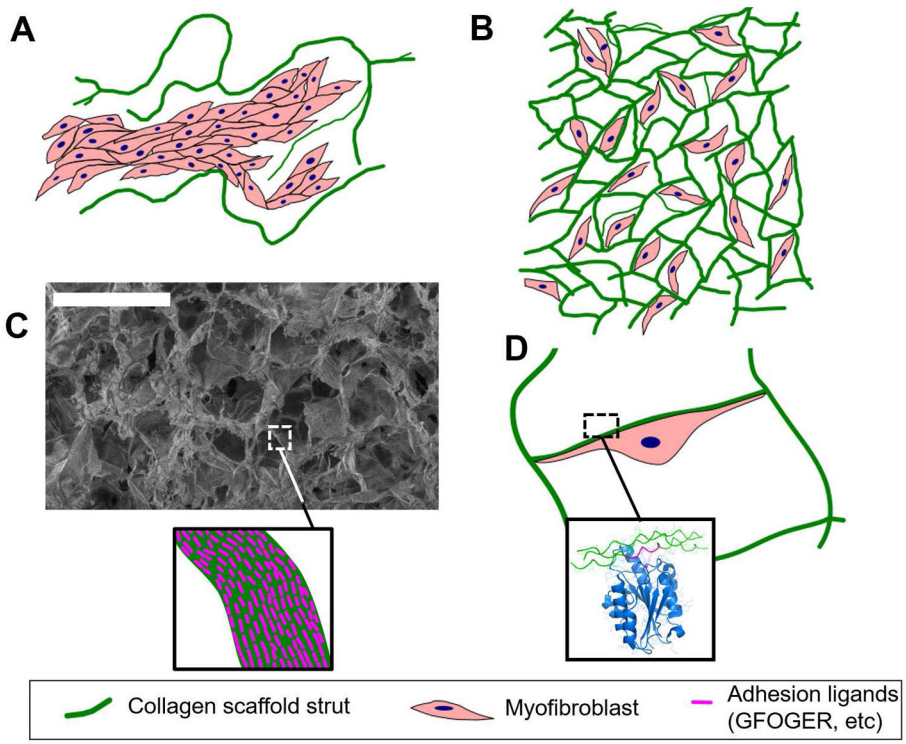

Figure 8.

Extensive cell binding to DRT, a biomaterial rich in adhesion ligands, is observed in biomaterial-induced regeneration, both in skin and peripheral nerves. A: In the case of a scaffold with very large pores (e.g., average pore size 400 μm, which does not induce regeneration), the low specific surface (surface per volume) of the material reduces the amount of adhesion ligands available per cell. In this case MFB bind to other MFB, forming large capsules inside the pores of the biomaterial rather than adhering to its surface. B: In the case of DRT (pore size approximately 100 μm, which induces regeneration), the mean pore diameter corresponds to a large specific surface and extensive cell-scaffold adhesion. MFB form few cell-cell contacts and do not form large capsules. C: The chemical stimuli provided by an active biomaterial to interacting cells depend both on the specific surface (SEM image shows the structure of a collagen scaffold of 90 μm mean pore diameter) and the surface chemistry of the scaffold (depicted in the insert as density of ligands of particular adhesion receptors, e.g. the GFOGER ligand for collagen-binding integrins). D: Illustration of a MFB interacting with the DRT surface. The extensive binding of each MFB on the DRT surface is mediated by binding of MFB adhesion receptors on the ligand-rich scaffold surface. For example, the insert depicts the binding of the I domain of integrin α_2 on the GFOGER ligand present in collagen molecules (rendering based on the crystal structure 1DZI).